Different Myofilament Nearest-Neighbor Interactions Have Distinctive Effects on Contractile Behavior

Maria V. Razumova,*‡ Anna E. Bukatina,*§ and Kenneth B. Campbell*†

Departments of *Veterinary and Comparative Anatomy, Physiology, and Pharmacology and †Biological Systems Engineering, Washington State University, Pullman, WA 99164; ‡Department of Physics, Division of Biophysics, Moscow State University, Moscow, Russia; and §Institute of Theoretical and Experimental Biophysics, Russian Academy of Sciences, Puschino, Russia

ABSTRACT Cooperativity in contractile behavior of myofilament systems almost assuredly arises because of interactions between neighboring sites. These interactions may be of different kinds. Tropomyosin thin-filament regulatory units may have neighbors in steric blocking positions (*off*) or steric permissive positions (*on*). The position of these neighbors influence the tendency for the regulatory unit to assume the on or off state. Likewise, the tendency of a myosin cross-bridge to achieve a force-bearing state may be influenced by whether neighboring cross-bridges are in force-bearing states. Also, a cross-bridge in the force-bearing state may influence the tendency of a regulatory unit to enter the *on* state. We used a mathematical model to examine the influence of each of these three kinds of neighbor interactions on the steady-state force-pCa relation and on the dynamic force redevelopment process. Each neighbor interaction was unique in its effects on maximal Ca^{2+}-activated force, position, and symmetry of the force-pCa curve and on the Hill coefficient. Also, each neighbor interaction had a distinctive effect on the time course of force development as assessed by its rate coefficient, k_{dev}. These diverse effects suggest that variations in all three kinds of nearest-neighbor interactions may be responsible for a wide variety of currently unexplained observations of myofilament contractile behavior.

INTRODUCTION

It is widely held that there is cooperativity among the contractile processes of the myofilament system (Weber and Bremel, 1972; Murray and Weber, 1980; Hill, 1985; Tobaccman 1996; Squire and Morris, 1998; Lehrer, 1994; McKillop and Geeves, 1993; Moss, 1992; Solaro and Rarick, 1998). Usually, cooperativity is understood operationally and is said to exist when the Hill coefficient in the fit to a binding isotherm is greater than 1. We prefer to consider cooperativity in conceptual terms where, by cooperativity, we mean that some event in the sequence of steps leading eventually to force production nonlinearly favors the occurrence of that same or other events in the sequence. There are many possibilities for cooperativity including (but not limited to) Ca^{2+} binding to Troponin C (TnC) enhancing the binding of more Ca^{2+} to TnC; the switching *on* of a thin filament regulatory complex favoring the switching *on* of other regulatory complexes; the formation of a force-bearing cross-bridge favoring the formation of more force-bearing cross-bridges; and any combination by which one of these (i.e., Ca^{2+} binding, switching on, and formation of force-bearing cross-bridges) nonlinearly favors another. In the highly structured myofilament system, cooperativity almost certainly implies some kind of interaction between neighboring locations along the length of the filaments. Of the various options, we chose to study three kinds of neighbor interactions that seemed likely contributors to cooperativity and that could yield insights from further investigation of their specific consequences.

The first of these was interaction between adjacent tropomyosin-troponin regulatory units, *RU*, on the thin filament: *RU-RU interaction.* In this, the tendency for an RU to transition from an *off* to an *on* state, or vice versa, depended on whether neighboring RUs were in the *on* or *off* states. The possibility for such interactions have been recognized for years, because RU tropomyosin backbones are stacked end-to-end along the length of the thin filament with an overlap of 5 to 10 residues (Tobaccman, 1996, Solaro and Rarick, 1998). In addition, the troponin T subunit of the RU extends over this overlap region, possibly to generate additional interactions between adjacent RUs. Interactions between adjacent RUs have been treated quantitatively in basic equilibrium theory (Hill, 1995), have been used in models to predict contractile behavior (Dobrunz et al., 1995; Rice et al., 1999), and have been used to explain seemingly grouped turning on of all activation sites along the thin filament (Brandt et al., 1984, 1987). Thus, RU-RU interactions are well recognized and studied, but quantitative studies of these effects relative to those of other types of neighbor interactions have not been performed.

The second neighbor interaction chosen was between adjacent cycling cross-bridges: *XB-XB interaction.* In this, the likelihood that a myosin XB will form an attachment to the thin filament and proceed to a force-bearing state is influenced by whether neighboring XBs are in force-bearing states. While direct experimental evidence for this kind of cooperativity cannot be cited, this mechanism is implicit in the thinking of many who have modeled cooperative interaction within the contractile system. Several of these pre-

Received for publication 1 July 1999 and in final form 11 February 2000.

Supported by National Institutes of Health Grant RO1 HL21462-20.

Address reprint requests to Dr. Kenneth Campbell, Washington State University, Dept. of VCAPP, Pullman, WA 99164. Tel.: 509-335-8011; Fax: 509-335-4650; E-mail: cvselkbc@vetmed.wsu.edu.

0006-3495/00/06/3120/18 $2.00

vious modeling efforts have considered XB-XB interactions only within the span of the 7 actin of a single RU as a result of steric relief secondary to tropomyosin displacement due to the first XB attachment within the RU span (Tobacman, 1996; Zou and Phillips, 1994; Rice et al., 1999). Other authors have implied that XB force causes filament stretch to bring about favorable alignment between the actin binding sites and the myosin XB to enhance the formation of more force-bearing XBs (Daniels et al., 1998; Mijailovich et al., 1996). Here, we do not specify a mechanism but consider only the potential phenomenon that one XB in a force-bearing state may enhance attachment and eventual force-bearing in an eligible neighboring XB (eligibility requires that the neighboring site must already be switched on). Our results will have qualitative relevance to what may be expected from any mechanism that operates to effectively bring about XB-XB cooperativity.

The third neighbor interaction studied was one in which an attached (force-bearing) cross-bridge facilitated the transition to the *on* state by a neighboring RU: *XB-RU interaction.* Again, this is a well appreciated cooperative interaction that has been implicated as the mechanism responsible for the activating actions of rigor bridges, of loose S1 myosin added to myofilament systems, and of apparent Ca^{2+}-independent activation at low ATP concentrations (Godt, 1974; Fitzsimons and Moss, 1998; Moss, 1992; Swartz et al., 1999; Swartz et al., 1996). Thus, although the evidence for this kind neighbor interaction is great, the peculiar contractile responses of XB-RU interaction that would distinguish it from, say, RU-RU or XB-XB interactions have never been documented.

The objective of this work was to contrast the effects on contraction of RU-RU, XB-XB, and XB-RU neighbor interactions. We used a mathematical model. Because our long term goal is to incorporate these neighbor interaction effects into a model for predicting nonequilibrium behaviors, such as will occur during a muscle twitch or a brief tetanus, we followed a kinetic approach to model development and did not adhere strictly to the constraints of equilibrium thermodynamics. This was necessary in order to separate the effects of individual neighbor interactions and to achieve mathematical tractability. The result is a model that captures the most relevant features of contractile processes and one that gives believable predictions of the essential consequences of these separate neighbor interaction effects.

Model Description

The model consisted of a kinetic core of RU with *on* and *off* states and XB with attached and detached states. Rate coefficients regulated steps in this kinetic core and were subject to change with neighbor interactions. The kinetic core and the neighbor interactions are discussed in turn.

Kinetic Core of Model

Consider the 8-state myofilament activation and cross-bridge cycling model in Fig 1. A portion of the thin filament is represented by the chain of three circles with the bar spanning the length of the chain. The myosin binding site on

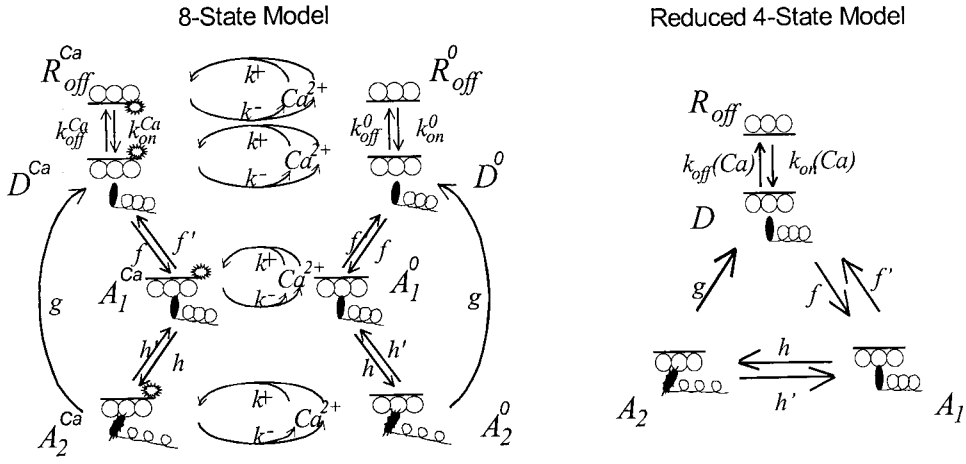

FIGURE 1 (Left) Eight-state cross-bridge activation and cycling model. A segment of the thin filament is represented by the chain of three circles. The thin-filament regulatory unit is represented by the bar associated with the 3-circle chain. The regulatory unit is in the *on* state when the bar is above the 3-circle chain and in the *off* state when the bar is below the chain. The myosin cross-bridge is represented by the shaded ellipse with the coiled tail. The cross-bridge may be detached (D) or attached (A_1, A_2) to the thin filament. In isometric conditions, force bearing is by the post-power stroke A_2 state. Calcium is bound to the regulatory unit by all states on the left half of the *left panel* and not bound to all states on the right half of the *left panel*. Superscripts indicate calcium-binding status. See text for definitions and detailed explanations. (Right) Reduced 4-state representation of 8-state model. Calcium binding and dissociation is now contained within the calcium dependence of the k_{on}(Ca) and k_{off}(Ca) rate coefficients.

actin is represented by the three circles (no stoichiometric relations are implied by the number three) and the regulatory tropomyosin-troponin unit (RU) controlling myosin access to the actin binding site is represented by the bar. The RU corresponds to a single tropomyosin-troponin complex. The myosin cross-bridge, XB, is represented by the shaded ellipse with the coiled tail. For the sake of simplicity, we assume a stoichiometry of 1 RU for every XB attachment site.

Ca^{2+} binds and dissociates from the low-affinity TnC site on the RU with rate constants of association, k^+, and dissociation, k^-. For simplicity, we consider just a single low-affinity Ca^{2+} binding site, as in cardiac muscle. Additionally, the RU may be in one of two steric configurations: the *off* position (states R_{off}^0 and R_{off}^{Ca}) or the *on* position (states D^0, D^{Ca}, A_1^0, A_1^{Ca}, A_2^0, and A_2^{Ca}). Switching between *off* and *on* positions is governed by the *on* rate constants, k_{on}^{Ca} and k_{on}^0, and the *off* constants, k_{off}^{Ca} and k_{off}^0, where the superscript indicates whether Ca^{2+} is bound to the RU. Ca^{2+} binding results in great differences between the two *on* constants, $k_{on}^{Ca} \gg k_{on}^0$, and also between the two *off* constants, $k_{off}^{Ca} \ll k_{off}^0$. When Ca^{2+} is not bound to TnC and the RU is *off* (state R_{off}^0), there is little probability that it will turn *on* ($k_{off}^0 \gg k_{on}^0$). When Ca^{2+} is bound to TnC, the *off* RU (state R_{off}^{Ca}) has an increasing probability of turning *on* ($k_{on}^{Ca} \gg k_{off}^{Ca}$).

The myosin binding site with the RU in the *on* state can be in one or more additional states depending on whether cross-bridges are attached or not. These include detached (D^0, D^{Ca}) and attached pre-power stroke (A_1^0, A_1^{Ca}) and attached post-power stroke (A_2^{Ca}, A_2^0). Cross-bridges can attach to the thin filament only when the RU is in the *on* configuration. Attachment, power stroke, and detachment occur cyclically according to rate constants f, f', h, h', and g, where f is the forward rate constant of cross-bridge attachment, h is the forward rate constant of the power stroke and g is the rate constant of cross-bridge detachment. Force is generated as cross-bridges go through the power stroke, i.e., transition from state A_1^{Ca} to state A_2^{Ca} and transition from state A_1^0 to state A_2^0. Ca^{2+} may bind and dissociate from TnC regardless of whether the RU is *on* or *off* and whether cross-bridges are attached or detached. When myosin heads are attached (A_1^0, A_1^{Ca}, A_2^0, and A_2^{Ca}), the RU has no probability to turn *off* and must await cross-bridge detachment before turning *off*.

By assuming that k^+ and k^- are large with respect to other rate coefficients, that these Ca^{2+}-binding constants are unaffected by whether the RU are on or off, and, further, that they are also independent of all events within the cross-bridge cycle, it is possible to reduce the 8-state model on the left-hand side of Fig. 1 to a 4-state model on the right-hand side of Fig. 1, where the states have been collapsed as follows:

$$R_{off} = R_{off}^0 + R_{off}^{Ca} \tag{1}$$

$$D = D^0 + D^{Ca} \tag{2}$$

$$A_1 = A_1^0 + A_1^{Ca} \tag{3}$$

$$A_2 = A_2^0 + A_2^{Ca} \tag{4}$$

In the reduced 4-state model, the rate constants for transitions between RU *on* and *off* states have a dependence on calcium, given by

$$k_{on} = k_{on}^0 + [k_{on}^{Ca} - k_{on}^0]\frac{Ca}{Ca_{50} + Ca} \tag{5}$$

$$k_{off} = k_{off}^0 + [k_{off}^{Ca} - k_{off}^0]\frac{Ca}{Ca_{50} + Ca} \tag{6}$$

where Ca_{50} ($= k^-/k^+$) is the calcium concentration of half Ca^{2+} saturation of thin filament binding sites.

By applying conservation to a fixed total number of actin-myosin sites, R_T, $R_T = R_{off} + D + A_1 + A_2$, three differential equations are all that are needed to describe the rate of change of states in the reduced, 4-state model.

$$\dot{D}(t) = k_{on}R_{off}(t) + f'A_1(t) + gA_2(t) - [k_{off} + f]D(t) \tag{7}$$

$$\dot{A}_1(t) = f\,D(t) + h'A_2(t) - [f' + h]A_1(t) \tag{8}$$

$$\dot{A}_2(t) = hA_1(t) - [h' + g]A_2(t) \tag{9}$$

States may be grouped into subpopulations. For instance, states D, A_1, and A_2 collectively represent a population of cycling XBs; state R_{off} represents a noncycling population. State A_2 is the only state that bears force during isometric conditions and, thus, isometric muscle force is proportional to the number of XBs in the A_2 state. For this reason, we use A_2 as a measure of force.

States and combinations of states may be expressed as fractions of R_T:

$$\lambda^{off} = \frac{R_{off}}{R_T} - \text{fraction of sites that are turned } \textit{off}. \tag{10}$$

$$\lambda^{on} = \frac{D + A_1 + A_2}{R_T} - \text{fraction of sites that are turned } \textit{on},$$

which also equals λ^{cyc}, the fraction of sites participating in XB cycling. (11)

$$\lambda^{D} = \frac{D}{R_T} - \text{fraction of sites in } D \text{ state}. \tag{12}$$

$$\lambda^{A_1} = \frac{A_1}{R_T} - \text{fraction of sites in } A_1 \text{ state}. \tag{13}$$

$$\lambda^{A_2} = \frac{A_2}{R_T} - \text{fraction of sites in } A_2 \text{ state}. \tag{14}$$

Now, states are distributed along the length of the thick filament. If that distribution is random, fractions given by Eqs. 10–14 represent the probability of finding a given

actin-myosin site in any particular state. In addition, it is useful to consider the fraction of cycling XBs that are generating force,

$$\lambda_{cyc}^{A_2} = \frac{A_2}{D + A_1 + A_2} \tag{15}$$

The goal of this work was to determine the effect of nearest neighbor RU and XB on k_{on}, k_{off}, f, and f' and the consequence of these effects on muscle contraction behavior. We consider only conditions of constant Ca^{2+} activation.

Nearest neighbor interactions

RU-RU interactions: interactions between neighboring regulatory units

Regulatory units are aligned head-to-tail along a thin filament. Any unit, whether in the off or on position, may have 4 possible nearest neighbor configurations, as in Fig 2: 1) both neighbors off, (= 11); 2) left neighbor off and right neighbor on, (= 12); 3) left neighbor on and right neighbor off, (= 21); and 4) both neighbors on (= 22).

Transitions between *on* and *off* are governed by k_{on} and k_{off}, which obey Boltzmann statistics,

$$k_{on}^{*} = k_a e^{-\frac{B_{12}^{\#}}{\kappa T}} \tag{16}$$

$$k_{off}^{*} = k_b e^{-\frac{B_{21}^{\#}}{\kappa T}} \tag{17}$$

where k_a and k_b are attempt frequencies; $B_{12}^{\#}$ and $B_{21}^{\#}$ are activation energies that need to be overcome to make the transition from state 1 (*off*) to 2 (*on*) and from state 2 to 1, respectively; # stands for any nearest-neighbor configuration; κ is the Boltzmann constant; and T is the absolute temperature. The exponential term, $e^{-(B_{ij}/\kappa T)}$, expresses the probability that an attempt to make a transition will be successful. The higher the activation energy, i.e., B_{ij}, the smaller the probability of success.

Turning on

End-to-end interactions between adjacent RU (perhaps through some mechanical coupling due to overlapping ends of tropomyosin and/or overlapping Tn-T) result in the state of the neighboring unit influencing the propensity of an *off* unit to make a transition to the *on* state (Fig. 3 *A*). Let this influence be exerted through the activation energy. Thus, for an RU in the *off* state, the activation energies associated with a state transition to the *on* state may be ordered:

$$B_{12}^{11} > B_{12}^{12} \approx B_{12}^{21} > B_{12}^{22} \tag{18}$$

where the superscripts refer to the states of the left and right neighbors and the ordering is the result of the influence of the left and right neighbor states on the activation energy required to make the transition. Thus, the success frequency (i.e., the rate constant for transition) from an *off* to an *on*

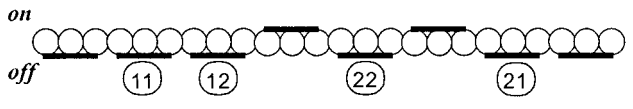

FIGURE 2 All possible thin filament regulatory unit nearest neighbor combinations: both neighbors are in *off* position (11), one neighbor in *on* and one in *off* (12 and 21), and both neighbors in *on* position (22).

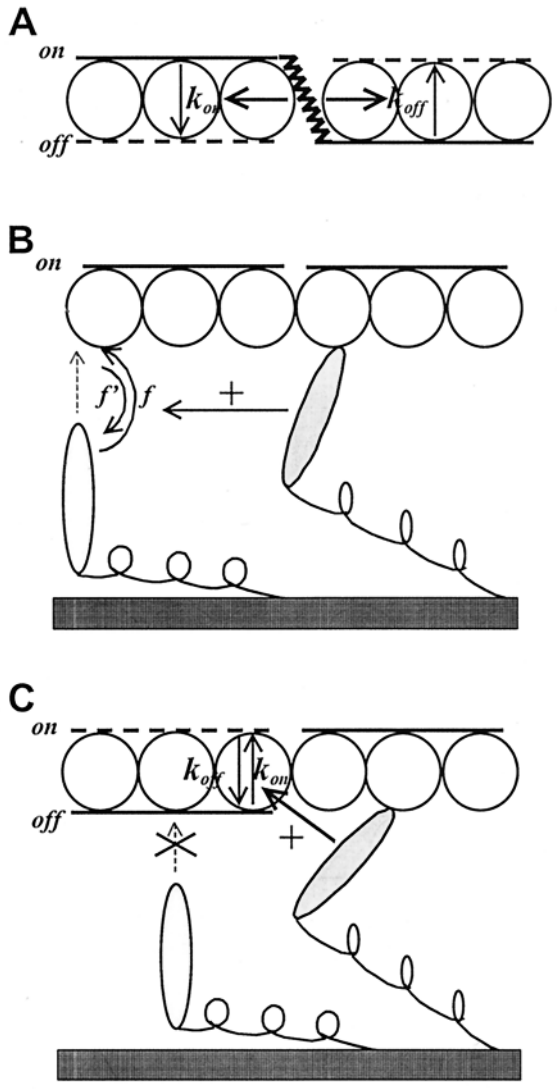

FIGURE 3 Three kinds of neighbor interactions. (*A*) Tethering between adjacent regulatory units results in the state of a neighboring unit influencing the propensity of an *off* unit to make a transition to the *on* state and an *on* unit to make a transition to *off* state. (*B*) Force-bearing XB facilitates the attachment of neighboring XB to the actin-binding site. (*C*) Force-bearing XB influences the on-off transition of neighboring thin filament regulatory unit.

state is greater as more neighbors assume the *on* state, because the activation energy that must be overcome for this transition declines as more neighbors turn *on*.

We may address this quantitatively by considering, for the whole population,

$$k_{on} = k_a\left\{\begin{bmatrix}\text{contribution by sites with}\\ \text{both neighbors "off"}\end{bmatrix} + \begin{bmatrix}\text{contribution by sites with}\\ \text{one neighbor "off" and one "on"}\end{bmatrix} + \begin{bmatrix}\text{contribution by sites with}\\ \text{both neighbors "on"}\end{bmatrix}\right\} \quad (19)$$

where k_a is an attempt frequency and the term in pointy brackets is the average probability over the whole population that an attempt will be successful. We estimated this average probability by taking the sum of weighted probabilities as follows. Weights were assigned using the assumption that events were randomly distributed along the length of the myofilament. (This is a far-reaching assumption with important consequences that are examined in detail in the Discussion.) With random distribution, the likelihood that a neighboring site will be in the *off* state is λ^{off} and the likelihood that it will be in the *on* state is λ^{on}. Joint likelihoods are given by the appropriate products as, for example, the likelihood that both neighboring sites will be *off* is $\lambda^{off}\lambda^{off}$, or that the right one will be *on* and the left one *off* is $\lambda^{on}\lambda^{off}$. Therefore, Eq. 19 may be written in quantitative terms as follows:

$$k_{on} = k_a\left\{\lambda^{off}\lambda^{off}e^{-\frac{B_{12}^{11}}{\kappa T}} + \lambda^{off}\lambda^{on}e^{-\frac{B_{12}^{12}}{\kappa T}} + \lambda^{on}\lambda^{off}e^{-\frac{B_{12}^{21}}{\kappa T}} + \lambda^{on}\lambda^{on}e^{-\frac{B_{12}^{22}}{\kappa T}}\right\} \quad (20)$$

Extracting $e^{-(B_{12}^{11}/\kappa T}$ out of the expression in brackets gives

$$k_{on} = k_a e^{-\frac{B_{12}^{11}}{kT}}\left((\lambda^{off})^2 + 2\lambda^{on}\lambda^{off}e^{-\frac{B_{12}^{12}-B_{12}^{11}}{\kappa T}} + (\lambda^{on})^2 e^{-\frac{B_{12}^{22}-B_{12}^{11}}{\kappa T}}\right) \quad (21)$$

Interaction between adjacent RUs impact the activation energy differences $B_{12}^{12} - B_{12}^{11}$ and $B_{12}^{22} - B_{12}^{11}$. Let this interaction be such that it reduces the activation energy required for an *off*-to-*on* transition by an amount U. Then,

$$\begin{aligned} B_{12}^{12} - B_{12}^{11} &= -U \\ B_{12}^{12} - B_{12}^{22} &= U \end{aligned} \quad (22)$$

Substituting these into Eq. 21 yields

$$k_{on} = k_a e^{-\frac{B_{12}^{11}}{kT}}\left((\lambda^{off})^2 + 2\lambda^{on}\lambda^{off}e^{\frac{U}{\kappa T}} + (\lambda^{on})^2 e^{\frac{2U}{\kappa T}}\right) \quad (23)$$

or

$$k_{on} = k_{on}^{u}\left(\lambda^{off} + \lambda^{on}e^{\frac{U}{\kappa T}}\right)^2 \quad (24)$$

where $k_{on}^{u} = k_a e^{-(B_{12}^{11}/\kappa T)}$ is a reference k_{on} coefficient for the condition where both neighbors are *off*. Note, because the effects of Ca^{2+} on k_{on} were taken independent of the effects of neighbor interactions, k_{on}^{u} incorporates the Ca^{2+} effect as given by Eq. 5.

Because $e^{(U/kT)}$ is simply a number, it may be given the value $u = e^{(U/kT)}$ such that if there is no effect from neighbor interaction, then $U = 0$ and $u = 1$. Furthermore, because $\lambda^{on} + \lambda^{off} = 1$, Eq. 24 can be rewritten as

$$k_{on} = k_{on}^{u}[1 + \lambda^{on}(u - 1)]^2 \quad (25)$$

The term in square brackets on the right-hand side indicates that if there are neighbor interactions (i.e., $u > 1$), then the value of k_{on} increases with increasing number of regulatory units in the *on* position.

Turning off

A similar analysis may be done to determine the average rate constant for the *on*-to-*off* transition. The relations are slightly reordered for the reverse transition such that

$$\begin{aligned} B_{21}^{12} - B_{21}^{11} &= U \\ B_{21}^{12} - B_{21}^{22} &= -U \end{aligned} \quad (26)$$

and, finally,

$$k_{off} = k_{off}^{u}[u - \lambda^{on}(u - 1)]^2 \quad (27)$$

where $k_{off}^{u} = k_b e^{-(B_{21}^{11}/\kappa T)}$ is the reference k_{off} coefficient for the condition where both neighbors are *off*. Note, because the effects of Ca^{2+} on k_{off} were taken independent of the effects of neighbor interactions, k_{off}^{u} incorporates the Ca^{2+} effect as given by Eq. 6.

The effects of interaction between neighbors on the *on*-to-*off* transition are slightly more complicated than on the *off*-to-*on* transition. If most RU are *off* (i.e., λ^{on} is small) the effect of u is to increase k_{off}. On the other hand, if most RU are *on* (i.e., λ^{on} is large) the effect of u is to decrease k_{off}.

Net Effect

The net effect of u on the transitions between *off* and *on* states can be appreciated from examining the ratio

$$\frac{k_{on}}{k_{off}} = \frac{k_{on}^{u}}{k_{off}^{u}}\left[\frac{1 + \lambda^{on}(u - 1)}{u - \lambda^{on}(u - 1)}\right]^2 \quad (28)$$

If λ^{on} is small (i.e., λ^{off} is large) as during low Ca^{2+}, increasing u decreases the k_{on}/k_{off} ratio and RU tend to be held in the *off* position as Ca^{2+} increases. However, if λ^{on}

is large, as during high Ca^{2+}, increasing u increases the k_{on}/k_{off} ratio and RU tend to be held in the *on* position as Ca^{2+} decreases.

XB-XB interactions: interactions between neighboring cross-bridges

A second interaction is the interaction between neighboring XB attachment sites. Neighboring actin-myosin attachment sites along the length of a thin filament will have a XB either attached or unattached. Transitions between unattached and attached states are governed by f and f' which, like k_{on} and k_{off}, obey Boltzmann statistics. As a beginning point, we consider that force-bearing in an attached state, whether A_1 or A_2, reduces the activation energy for a D-to-A_1 transition and thus, increases the rate coefficient f while decreasing the reverse rate coefficient, f' (Fig. 3 *B*). In the isometric conditions we study here, force generation occurs only in the A_2 state. Thus in the way we have set up this problem, whether force from the A_2 state is used as the variable that reduces the activation energy or strong binding is used as that variable, there will be no difference in the resulting formulation of f and f'. Equivalence between force and strong binding would not be the case during either shortening or stretching when force in the A_2 state would depend on both its strong binding and its altered distortion (Razumova et al., 1999) and XBs in the A_1 state would also generate force. Shortening and stretching are not investigated here; therefore, whether force generation or strong binding is the important variable in these interaction effects remains an issue for a future study.

In a manner similar to that followed for k_{on} and k_{off}, we can write

$$f = f_a\Big\{\Big[\text{contribution by sites with neighbors neither of which has a force-bearing XB}\Big] + \Big[\text{contribution by sites with neighbors one of which has a force-bearing XB}\Big] + \Big[\text{contribution by sites with neighbors both of which have a force-bearing XB}\Big]\Big\} \quad (29)$$

where f_a is an attempt frequency and the term inside the pointy brackets represents the population average of the probability of a successful transition. The likelihood that a neighboring site will be: i) unattached is $\lambda^{off} + \lambda^{D}$, ii) attached and in the A_1 state is λ^{A_1}, and iii) attached and in the A_2 state is λ^{A_2}. Joint likelihoods are given by the appropriate product; for example, the likelihood that both neighboring sites will be unattached is $(\lambda^{off} + \lambda^{D})(\lambda^{off} + \lambda^{D})$. Therefore, Eq. 29 may be written in quantitative terms as follows:

$$f = f_a\Big\{(\lambda^{off} + \lambda^{D})(\lambda^{off} + \lambda^{D})e^{-\frac{B^{00}_{DA_1}}{kT}} + 2(\lambda^{off} + \lambda^{D})\left(\lambda^{A_1}e^{-\frac{B^{0A_1}_{DA_1}}{kT}} + \lambda^{A_2}e^{-\frac{B^{0A_2}_{DA_1}}{kT}}\right) + \left(\lambda^{A_1}\lambda^{A_1}e^{-\frac{B^{A_1A_1}_{DA_1}}{kT}} + 2\lambda^{A_1}\lambda^{A_2}e^{-\frac{B^{A_1A_2}_{DA_1}}{kT}} + \lambda^{A_2}\lambda^{A_2}e^{-\frac{B^{A_2A_2}_{DA_1}}{kT}}\right)\Big\} \quad (30)$$

where the $B^{xy}_{DA_1}$ are the respective activation energies associated with a D-to-A_1 transition for the respective xy neighbor conditions. The superscript "0" refers to the non-force-bearing state, be it D or R_{off}. Taking the $B^{00}_{DA_1}$ as a reference value and factoring it outside the pointy brackets yields

$$f = f_a e^{-\frac{B^{00}_{DA_1}}{kT}}\Big[(\lambda^{off} + \lambda^{D})(\lambda^{off} + \lambda^{D}) + 2(\lambda^{off} + \lambda^{D})\left(\lambda^{A_1}e^{-\frac{B^{0A_1}_{DA_1} - B^{00}_{DA_1}}{kT}} + \lambda^{A_2}e^{-\frac{B^{0A_2}_{DA_1} - B^{00}_{DA_1}}{kT}}\right) + \left(\lambda^{A_1}\lambda^{A_1}e^{-\frac{B^{A_1A_1}_{DA_1} - B^{00}_{DA_1}}{kT}} + 2\lambda^{A_1}\lambda^{A_2}e^{-\frac{B^{A_1A_2}_{DA_1} - B^{00}_{DA_1}}{kT}} + \lambda^{A_2}\lambda^{A_2}e^{-\frac{B^{A_2A_2}_{DA_1} - B^{00}_{DA_1}}{kT}}\right)\Big] \quad (31)$$

Assuming a mechanical mechanism, it is reasonable that the reduction in activation energy is proportional to the force in the cross-bridge at the neighboring site, and we can write

$$B^{0A_1}_{DA_1} - B^{00}_{DA_1} = -V\cdot F_{A_1} \quad (32)$$

$$B^{0A_2}_{DA_1} - B^{00}_{DA_1} = -V\cdot F_{A_2} \quad (33)$$

$$B^{A_1A_1}_{DA_1} - B^{00}_{DA_1} = -V\cdot (F_{A_1} + F_{A_1}) \quad (34)$$

$$B^{A_1A_2}_{DA_1} - B^{00}_{DA_1} = -V\cdot (F_{A_1} + F_{A_2}) \quad (35)$$

$$B^{A_2A_2}_{DA_1} - B^{00}_{DA_1} = -V\cdot (F_{A_2} + F_{A_2}) \quad (36)$$

where V is the constant of proportionality and the F_{A_1} and F_{A_2} are the forces associated with the respective attached XBs at neighboring sites. Rearrangement gives

$$f = f_a e^{-\frac{B^{00}_{DA_1}}{kT}}\Big[(\lambda^{off} + \lambda^{D})(\lambda^{off} + \lambda^{D}) + 2(\lambda^{off} + \lambda^{D})\left(\lambda^{A_1}e^{\frac{VF_{A_1}}{kT}} + \lambda^{A_2}e^{\frac{VF_{A_2}}{kT}}\right) + \left(\lambda^{A_1}\lambda^{A_1}e^{\frac{2VF_{A_1}}{kT}} + 2\lambda^{A_1}\lambda^{A_2}e^{\frac{V(F_{A_1}+F_{A_2})}{kT}} + \lambda^{A_2}\lambda^{A_2}e^{\frac{2VF_{A_2}}{kT}}\right)\Big] \quad (37)$$

We make the assignment $f_0 = f_a e^{-(B^{00}_{DA_1}/kT)}$ where f_0 is a reference value that refers to the condition when no neighbors are in the force-bearing state. Applying the identity $\lambda^{off} + \lambda^{D} + \lambda^{A_1} + \lambda^{A_2} = 1$ and substituting gives

$$f = f_0\Bigg[(1 - \lambda^{A_1} - \lambda^{A_2})^2 + 2(1 - \lambda^{A_1} - \lambda^{A_2}) \cdot \left(\lambda^{A_1} e^{\frac{VF_{A_1}}{kT}} + \lambda^{A_2} e^{\frac{VF_{A_2}}{kT}}\right) + \left(\lambda^{A_1} e^{\frac{VF_{A_1}}{kT}} + \lambda^{A_2} e^{\frac{VF_{A_2}}{kT}}\right)^2\Bigg] \quad (38)$$

According to elastic cross-bridge theory and arguments we have made previously (Razumova et al., 1999), $F_{A_1} = \xi x_1$ and $F_{A_2} = \xi x_2$ where ξ is the stiffness of a single cross-bridge and x_1 and x_2 are the average distortions among the respective A_1 and A_2 cross-bridge states. Under the isometric conditions being considered here, $x_1 = 0$ and $x_2 = x_0$ where x_0 is the average distortion among A_2 XBs. This distortion may be visualized as being induced during the power stroke by head rotation. Terms in the exponent may be collected into a number, $\xi(V/kT)x_0$, that varies only with the magnitude of neighboring XB-XB interactions. We choose to give this number the value $v - 1$, where v now represents an arbitrary parameter that weights the strength of neighboring XB-XB interaction. When $v = 1$, there is no interaction; when $v > 1$ there is interaction. Thus, we may write, in general,

$$f = f_0\left[1 + \lambda^{A_1}\left(e^{(v-1)\frac{x_1}{x_0}} - 1\right) + \lambda^{A_2}\left(e^{(v-1)\frac{x_2}{x_0}} - 1\right)\right]^2 \quad (39)$$

which, during isometric conditions, reduces to

$$f = f_0[1 + \lambda^{A_2}(e^{(v-1)} - 1)]^2 \quad (40)$$

In a manner similar to that used for the reverse coefficient in the k_{on}-to-k_{off} transitions, it can be shown that

$$f' = f'_0\left[1 + \lambda^{A_1}\left(e^{-(v-1)\frac{x_1}{x_0}} - 1\right) + \lambda^{A_2}\left(e^{-(v-1)\frac{x_2}{x_0}} - 1\right)\right]^2 \quad (41)$$

which, under isometric conditions, reduces to

$$f' = f'_0[1 + \lambda^{A_2}(e^{-(v-1)} - 1)]^2 \quad (42)$$

Thus, increasing the interaction between neighboring XBs by increasing the parameter v increases f and reduces f'. Both these actions increase the ratio

$$\frac{f}{f'} = \frac{f_0}{f'_0}\left[\frac{1 + \lambda^{A_2}(e^{(v-1)} - 1)}{1 + \lambda^{A_2}(e^{-(v-1)} - 1)}\right]^2 \quad (43)$$

and shift XBs from the detached to the attached states.

XB-RU interactions: interaction between a regulatory unit and neighboring cross-bridges

A third kind of neighbor interaction is one in which the *off*-to-*on* transition of an RU is favored by force-bearing in a XB at a neighboring actin-myosin attachment site. This is depicted in Fig. 3 *C*. We allow that force-bearing by a XB at the neighboring site reduces the activation energy required for an *off*-to-*on* transition and we proceed much as before to consider a whole population of regulatory units. The average k_{on} for the entire population will be the sum of weighted k_{on} values of all the transitions for each of the nearest neighbor configurations, as below:

$$k_{on} = k_a\Bigg\{\begin{bmatrix}\text{contribution by sites with}\\ \text{neighbors neither of which has a}\\ \text{force-bearing XB}\end{bmatrix} + \begin{bmatrix}\text{contribution by sites with}\\ \text{neighbors one of which has a}\\ \text{force-bearing XB}\end{bmatrix} + \begin{bmatrix}\text{contribution by sites with}\\ \text{neighbors both of which have a}\\ \text{force-bearing XB}\end{bmatrix}\Bigg\} \quad (44)$$

where k_a is the attempt frequency and the sum of terms inside the pointy brackets represents the population average of the probability of a successful transition. As before, Eq. 44 is written quantitatively as

$$k_{on} = k_a\Bigg\{(\lambda^{off} + \lambda^{D})\,(\lambda^{off} + \lambda^{D})e^{-\frac{B^{00}_{12}}{kT}} + 2(\lambda^{off} + \lambda^{D})\left(\lambda^{A_1} e^{-\frac{B^{0A_1}_{12}}{kT}} + \lambda^{A_2} e^{-\frac{B^{0A_2}_{12}}{kT}}\right) + \left(\lambda^{A_1}\lambda^{A_1} e^{-\frac{B^{A_1A_1}_{12}}{kT}} + 2\lambda^{A_1}\lambda^{A_2} e^{-\frac{B^{A_1A_2}_{12}}{kT}} + \lambda^{A_2}\lambda^{A_2} e^{-\frac{B^{A_2A_2}_{12}}{kT}}\right)\Bigg\} \quad (45)$$

where the B^{xy}_{12} are the respective activation energies associated with an *off*-to-*on* transition for the respective *xy* neighbor conditions.

If the reduction in activation energy is by some kind of mechanical mechanism, then it is reasonable that this reduction depends on the amount of force in the XB at the neighbor site, and we can write

$$B^{0A_1}_{12} - B^{00}_{12} = -W \cdot F_{A_1} \quad (46)$$

$$B^{0A_2}_{12} - B^{00}_{12} = -W \cdot F_{A_2} \quad (47)$$

$$B^{A_1A_1}_{12} - B^{00}_{12} = -W \cdot (F_{A_1} + F_{A_1}) \quad (48)$$

$$B^{A_1A_2}_{12} - B^{00}_{12} = -W \cdot (F_{A_1} + F_{A_2}) \quad (49)$$

$$B^{A_2A_2}_{12} - B^{00}_{12} = -W \cdot (F_{A_2} + F_{A_2}) \quad (50)$$

where W is a constant of proportionality and F_{A_1} and F_{A_2} are the forces associated with the respective attached XBs at neighboring sites. We proceed as we did with force-bearing effects on f to get

$$k_{on} = k_{on}^{w}\left[1 + \lambda^{A_1}\left(e^{(w-1)\frac{x_1}{x_0}} - 1\right) + \lambda^{A_2}\left(e^{(w-1)\frac{x_2}{x_0}} - 1\right)\right]^2 \quad (51)$$

where $k_{on}^{w} = k_a e^{-(B_{12}^{00}/kT)}$ represents a reference value when there is no XB attachment at neighboring sites (different from k_{on}^{u}) and $(w - 1) = \xi(W/kT)x_0$ is a number that varies with the magnitude of neighboring XB-RU interactions. When $w = 1$, there is no interaction; when $w > 1$ there is interaction. During isometric contraction, Eq. 51 reduces to

$$k_{on} = k_{on}^{w}[1 + \lambda^{A_2}(e^{(w-1)} - 1)]^2 \quad (52)$$

As before, it can be shown that under isometric conditions,

$$k_{off} = k_{off}^{w}[1 + \lambda^{A_2}(e^{-(w-1)} - 1)]^2 \quad (53)$$

Thus, increasing the interaction between XB-RU neighbors by increasing the parameter w increases k_{on} and reduces k_{off}.

Model Summary

In summary, the essential kinetics of activation and cross-bridge cycling were represented as a 4-state RU-XB model which, after applying a conservation constraint, was described by three differential equations (Eqs. 7–9). The effects of calcium to activate RU were represented algebraically (Eqs. 5 and 6). Three kinds of neighbor interactions resulted in nonlinear expressions for the *on* and *off* RU rate coefficients (Eqs. 25–28, 52, and 53) and the rate coefficients governing the XB attachment step (Eqs. 41–43). Single parameters allowed gradation of each neighbor interaction. Taken together, these equations constituted a nonlinear, third-order dynamic model in the state variables D, A_1, and A_2.

In these studies, all inputs to the model were held constant and dynamic behavior was the result of responses to non-steady-state initial conditions. Model output was a predicted force that, under the isometric conditions of these simulated experiments, was proportional to A_2. The model contained 14 parameters, including 10 reference values for the rate coefficients (k_{on}^0, k_{on}^{Ca}, k_{off}^0, k_{off}^{Ca}, Ca_{50}, f_0, f_0', h, h', g); an index for total number of actin-myosin reaction sites (R_T), and 3 parameters for grading each of the three kinds of neighbor interaction (u, v, w). Parameters used in this study were taken from an earlier study (Razumova et al., 1999) where it was found that the values given in Table 1 gave good reproductions of dynamic complex stiffness, step response, and force-velocity behavior as signatures of merit for dynamic contractile system behavior. Other values may be equally good, but those of Table 1 were found to be suitable reference values.

TABLE 1 Reference model parameters (s^{-1})

k_{on}^0	k_{on}^{Ca}	k_{off}^0	k_{off}^{Ca}	f_0	f_0'	h	h'	g	R_T
0	120	100	50	50	400	8	6	4	1

Methods

To meet the objective of contrasting the effects of RU-RU, XB-XB, and XB-RU neighbor interactions on contraction, the model was solved to predict steady-state force during varying levels of constant Ca^{2+} activation, yielding force-log (Ca/Ca_{50}) curves, and to predict the time course of force development starting from zero-force initial conditions, yielding characteristic time of force development. Given the complexity of the model equations, it was most practical to solve the model for any given set of parameters by assigning initial conditions to the state variables (D, A_1, A_2) and then numerically integrating the differential equations until steady state was obtained. Numerical integration was by a fourth-order Runge-Kutta methods using an integration step size of 0.1 ms. All programs were written in Fortran and Visual Basic and computations were performed on a Pentium II 400MHz computer.

Force-log(Ca/Ca_{50})

Ca^{2+} change was simulated by changing the Ca/Ca_{50} ratio between 0.01 and 100. The steady-state value of force predicted by the model was found for each Ca/Ca_{50} value and the resulting force-log(Ca/Ca_{50}) curve was plotted. This was done for the baseline parameters of Table 1; i.e., no neighbor interactions and no cooperativity. Then, the parameters grading the strength of neighbor interactions were individually changed to give in each case moderate and strong interactions and corresponding force-log(Ca/Ca_{50}) curves for these conditions were obtained. Care was taken to avoid values of interaction parameters that predicted phase transition in this system (see Discussion). Features of force-log(Ca/Ca_{50}) curve were evaluated and compared among the various conditions. Features compared included: force during maximal Ca^{2+} activation, F_{max}; log(Ca/Ca_{50}) at half F_{max}; Hill coefficient, n_H, of the Hill equation fitted to the model-predicted force-log(Ca/Ca_{50}) curve

$$F = \frac{1}{1 + \left(\frac{Ca}{Ca_{50}}\right)^{-n_H}}$$

and measures of curve asymmetry. Curve asymmetry was assessed by contrast of Hill coefficient for fit to relationship over range $F/F_{max} < 0.5$ *vs.* that for fit to relationship over

the range $F/F_{max} > 0.5$. In many cases, it was not possible to find one value for n_H for the whole curve, even when the curve was symmetrical. In these situations, three values of n_H are reported: one representative of the rising part of the force-log(Ca/Ca_{50}), one representative of the middle part, and one representative of the approach to saturation.

Force redevelopment

To determine the impact of neighbor interactions on dynamic behavior, we evaluated the model-predicted time course and characteristic time of force development at constant Ca^{2+} activation. The experimental approach to this measurement is to release and restretch a constantly activated muscle preparation in an attempt to create zero force by breaking all attached XBs. Then the time course of force rise to some steady state is observed and characterized with a single exponential rate constant, k_{tr}. We simulated the experimental force development episode by setting the initial value of the force-bearing A_2 state to zero and then predicted the time course of force development. We found that the force development transient was largely insensitive to the initial values given to A_1 and D and, thus, these too were routinely set to zero at the beginning of the force development period. A characteristic rate constant of force redevelopment, k_{dev}, was calculated by taking the reciprocal of the time required to reach $(1 - 1/e)F_{max}$. This was evaluated for several values of the neighbor interaction parameters.

For a monoexponential process, $k_{dev} = k_{tr}$. However, in many cases the time course of force redevelopment (both experimental observation and model prediction) cannot be well fitted with a simple monoexponential. To avoid curve fitting problems, we chose the operational definition given above.

RESULTS

RU-RU interactions

Increasing the strength of RU-RU interactions by increasing u from 1 (no interaction) to 3 (strong interaction) increased the maximum Ca^{2+}-activated force by approximately 30% (Fig. 4 *A*, Table 2). Concurrent changes in λ^{cyc}, $\lambda_{cyc}^{A_2}$, and λ^{A_2} at maximum Ca^{2+}-activated force are given in Table 2. In addition, increases in u increased the steepness of the force-logCa curve, n_H increased from 1 ($u = 1$, one coefficient for the whole curve) to 2-12-3 ($u = 3$, three coefficients for fits to low, middle, and upper parts of curve; Fig. 4 *B*). This increase in steepness was associated with a shift of the curve that may be described as a right shift for $F/F_{max} < 0.75$ and a left shift for $F/F_{max} > 0.75$ (Fig. 4 *B*). Associated with the right shift portion of the curve was a decrease in the k_{on}/k_{off} ratio relative to that for a given log (Ca/Ca_{50}) at $u = 1$ while associated with the left shift portion of the curve was a corresponding increase in the k_{on}/k_{off} ratio. The right shift in the lower part of the curve was so pronounced as to cause a net shift 0.35 pCa units to the right at $F/F_{max} = 0.5$.

At maximal Ca^{2+} activation, u had a nondiscernible effect on k_{dev}. Under conditions of low Ca^{2+} activation, u had a slight effect to slow force development and reduce k_{dev} (data not shown).

XB-XB interactions

Increasing the strength of XB-XB interaction from $v = 1$ (no interaction) to $v = 3.2$ (strong interaction) increased the maximum Ca-activated force, F_{max}, by approximately 6.5 times (Fig. 5 *A*). Unlike the effect with RU-RU interactions,

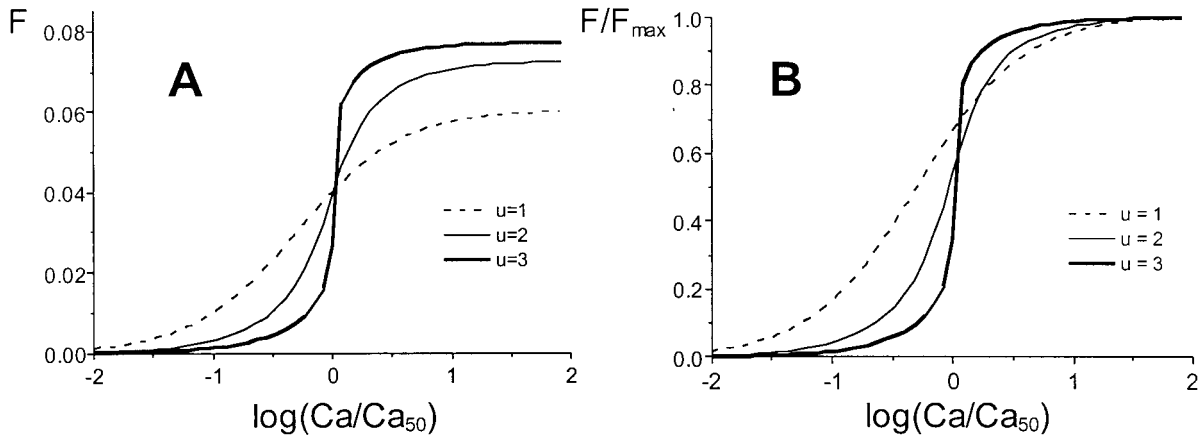

FIGURE 4 RU-RU interaction effect on force-pCa. Three curves represent different strength of interaction: no interaction (*dashed curve*, $u = 1$), weak interaction (*thin curve*, $u = 2$), and strong interaction (*thick curve*, $u = 3$). (*A*) Absolute values. (*B*) Normalized curves. Increasing strength of RU-RU interaction increases maximal Ca^{2+}-activated force, shifts the curve predominantly to the right (especially at low Ca^{2+}), increases curve steepness, and introduces curve asymmetry (relatively slow departure from no-force baseline, rapid approach to saturation).

TABLE 2 Results summary

Interaction parameters			At maximal Ca^{2+} activation							Force-log(Ca/Ca_{50})	
u	v	w	$\frac{k_{on}}{k_{off}}$	$\frac{f}{f'}$	$\frac{F_{max}}{F_{max0}}$	λ^{cyc}	$\lambda^{A_2}_{cyc}$	λ^{A_2}	k_{dev}	n_H	$\Delta[\log (Ca/Ca_{50})]_{50}$
1	1	1	2.4	0.125	1	0.75	0.08	0.06	10	1	0
3	1	1	17	0.125	1.3	0.95	0.08	0.08	10	2-12-3	0.35
1	3.2	1	2.4	4.7	6.5	0.96	0.40	0.38	2.4	2-7-2	0.1
1	1	5	80	0.125	1.3	0.99	0.08	0.08	10	3; 1.5	−0.9

the percentage of cycling cross-bridges that were in the force-bearing state at maximal Ca^{2+} activation increased dramatically with increased v from $\lambda^{A_2}_{cyc} = 0.08$ when $v = 1$ to $\lambda^{A_2}_{cyc} = 0.4$ when $v = 3.2$. Concurrently, the percentage of all cross-bridges that had been recruited into the cycling population also increased from $\lambda^{cyc} = 0.75$ when $v = 1$ to $\lambda^{cyc} = 0.96$ when $v = 3.2$.

The steepness of the force-log(Ca/Ca_{50}) curve exhibited a nonsystematic increase with increases in v; there was no change in n_H from the value 1 as v increased from 1 to 2.5 but a large increase to three-part value 2-7-2 when $v = 3.2$ (Fig. 5 *B*). These changes with v were associated with a right shift of the normalized force-log(Ca/Ca_{50}) curve as long as there were no changes in n_H. But when increasing v caused n_H to increase, the right-shifted curve began to move back to the left as it became steeper.

Unlike the effects of u, v had a strong effect on the rate of force development (Fig. 6). Increasing v decreased k_{dev}; $k_{dev} = 10\ sec^{-1}$ when $v = 1$ and $k_{dev} = 2.4\ sec^{-1}$ when $v = 3$. These pronounced effects are secondary to changes in f/f' for reasons elaborated in the Discussion.

XB-RU interaction

As with increasing u and v, increasing the strength of XB-RU interaction increased F_{max}. Increasing w from 1 (no interaction) to 5 (strong interaction) increased the maximum Ca^{2+}-activated force, F_{max}, by approximately 30% (Fig. 7 *A*). The magnitude of these effects was more like for u than for v.

However, unlike either u or v, increasing w caused a dramatic left shift in the normalized force-log(Ca/Ca_{50}) curve (Fig. 7 *B* and Table 2). The left-shifted curve was not symmetrical, having a higher n_H in the lower part ($n_H = 3$) than in the upper part ($n_H = 1.5$).

Similar to u, at maximal Ca^{2+} activation w had very little effect on the rate of force development, k_{dev}.

Combined effects on rate of force development

Although u and w alone had no significant effect on k_{dev} at maximal Ca^{2+} activation, in combination with v they produced non-additive effects that could not be anticipated. For

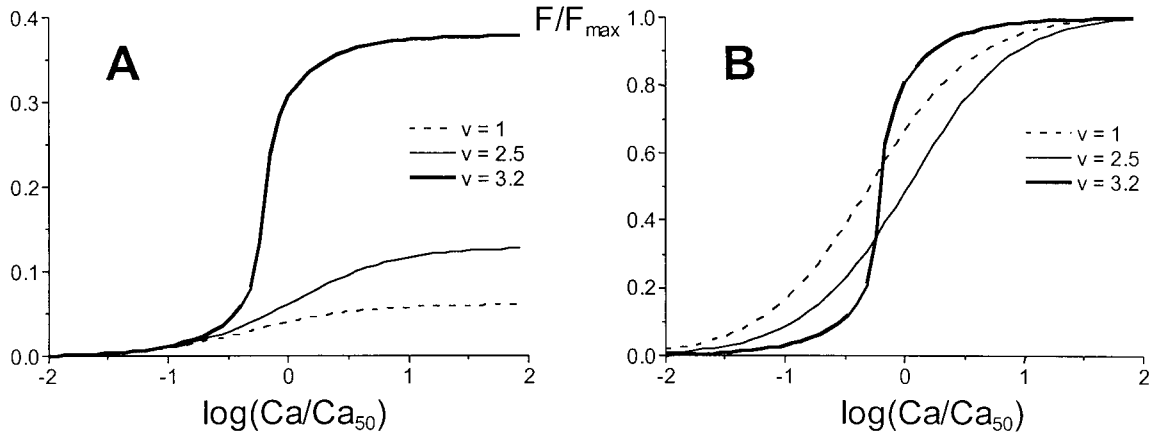

FIGURE 5 XB-XB interaction effect on force-pCa. Three curves represent different strength of interaction: no interaction (*dashed curve*, $v = 1$), weak interaction (*thin curve*, $v = 2.5$), and strong interaction (*thick curve*, $v = 3.2$). (*A*) Absolute values. (*B*) Normalized curves. Increasing strength of XB-XB interaction greatly increases maximal Ca^{2+}-activated force, shifts the curve to the right with weak interaction, increases curve steepness only with strong interaction, and introduces distinct curve asymmetry (relatively rapid departure from no-force baseline, slower approach to saturation).

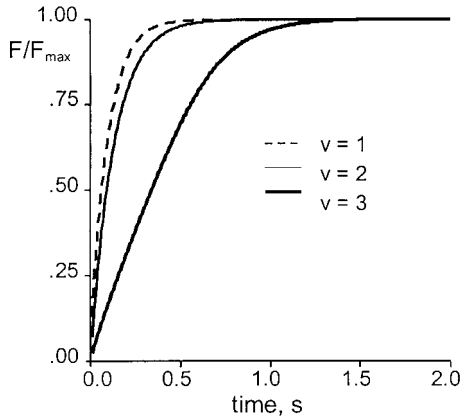

FIGURE 6 XB-XB interaction effect on time-course of force redevelopment. Three curves represent different strength of interaction: no interaction (*dashed curve*, $v = 1$), weak interaction (*thin curve*, $v = 2$), and strong interaction (*thick curve*, $v = 3$). Force axis normalized to the maximum value. Increasing strength of XB-XB interaction slows force redevelopment.

example, when the parameter set was ($u = 1$, $v = 3$, $w = 1$), k_{dev} was 2.4 s^{-1}. However, for either ($u = 3$, $v = 3$, $w = 1$) or ($u = 1$, $v = 3$, $w = 3$), k_{dev} was 4 s^{-1} (Fig. 8). Thus, adding a u or a w effect to an already existing v effect resulted in an unanticipated increase in the speed of force development.

DISCUSSION

The most important finding of these studies is that different and varied contractile behaviors can be generated with three different types of myofilament neighbor interactions. For instance, whereas increased strength of RU-RU, XB-XB, and XB-RU neighbor interactions all increased maximal Ca^{2+}-activated force, the magnitudes of these increases and the Ca^{2+}-dependent approach to maximal Ca^{2+}-activated force varied markedly among the three interaction types (Figs. 4, 5, and 7). Additionally, the nature and magnitude of effects on speed of force development also varied among neighbor interaction types. A second important finding was that large changes in the force-log(Ca/Ca_{50}) curves, including large shifts in the apparent Ca^{2+} sensitivity, can be obtained with these interactions with no change in the binding of Ca^{2+} to troponin. Explanations for the nature of and differences between effects are found in the nonlinear characteristics of the interactions and their relation to the overall model.

Critique of the model

All models are overt simplifications; the current model is no exception. For instance, we considered RUs and XBs interacting only along a single thin filament and ignored interactions that may occur among multiple thick and thin filaments as, for instance, changes in filament lattice spacing and its effect on interactions during force development and length change. A partial list of other factors that were ignored include: 1) end effects (we assumed an infinitely long thin filament); 2) restrictions due to spacing between actin attachment sites along thin filaments and XB spacing along thick filaments; 3) compliant properties of thick and thin filaments; 4) steric relations that allow one RU, in spanning 7 actin monomers, to regulate the availability of as many as three XB attachment sites on the thin filament; 5) more than one Ca^{2+} regulatory binding site on an RU; 6) all length-dependent activation phenomena; 7) states of an RU other than *on* or *off*; 8) the multiple states within the XB

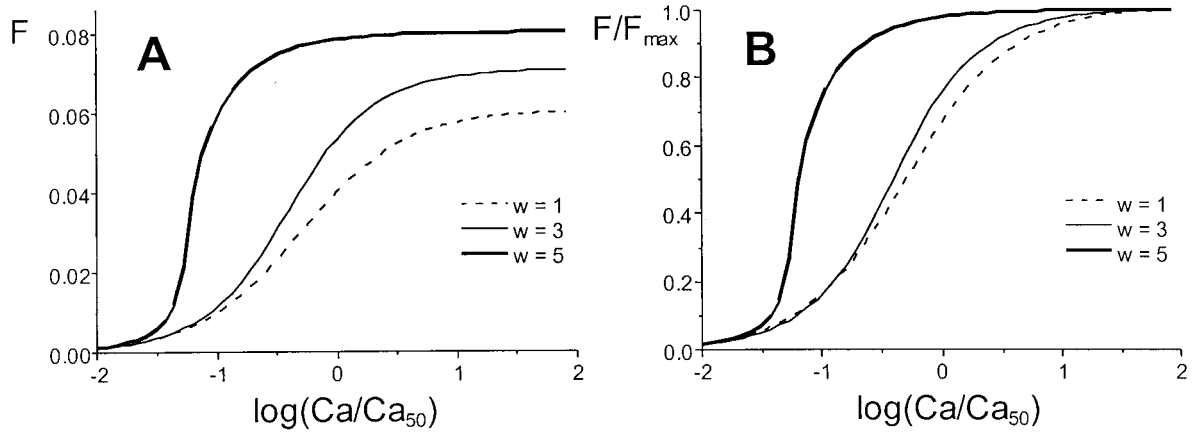

FIGURE 7 XB-RU interaction effect on force-pCa. Three curves represent different strength of interaction: no interaction (*dashed curve*, $w = 1$), weak interaction (*thin curve*, $w = 3$), and strong interaction (*thick curve*, $w = 5$). (*A*) Absolute values. (*B*) Normalized curves. Increasing strength of XB-RU interaction modestly increases maximal Ca^{2+}-activated force, shifts the curve strongly to the left, increases curve steepness, and introduces distinct curve asymmetry (relatively rapid departure from no-force baseline, slower approach to saturation).

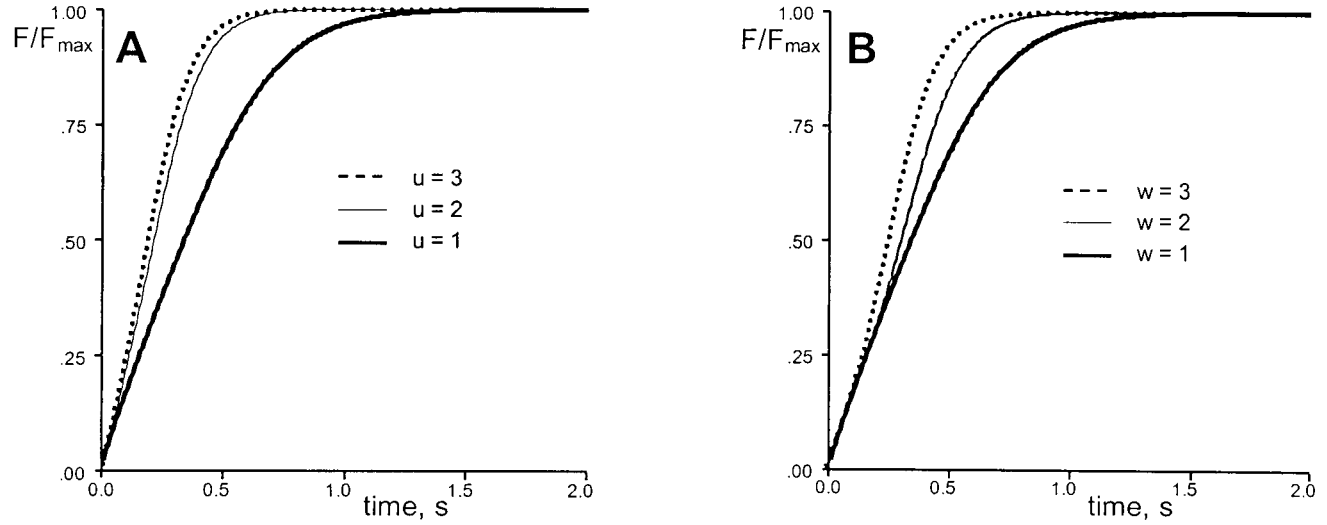

FIGURE 8 Effect of two simultaneous nearest-neighbor interactions on time course of force development. In both A and B there is a background of strong XB-XB interaction ($v = 3$). (*A*) On top of the background XB-XB interaction, varying strengths of RU-RU interaction are added ($u = 1$, 2, and 3). (*B*) On top of the background XB-XB interaction, varying strengths of XB-RU interaction are added ($w = 1$, 2, and 3). In the presence of a background of XB-XB interaction, the addition of either RU-RU interaction or XB-RU interaction causes a speeding of the force development process.

cycle; and 9) many other complicating factors that are known to exist within the myofilament system and the regulated interaction between actin and myosin. All assumptions were made to allow focus on specific phenomena and in order to keep the problem tractable.

Of the many assumptions, it is worth noting that treating the RU as either *on* or *off* does not incorporate the full range of subtleties that would come from direct interactions between RU and XB at a single binding site as implied in the 3 RU-state model (*blocked, closed*, and *open*) of Geeves and coworkers (McGillop and Geeves, 1993; Leher, 1994; Geeves and Leher, 1994). A rough equivalence between the 3 RU-state scheme and the one used here is as follows: *blocked* would be equivalent to our R_{off}, *closed* would be equivalent to an equilibrium combination of D and A_1, and *open* would be equivalent to an equilibrium combination of D and A_2. The transition between *blocked* and *closed* would be associated with Ca^{2+} binding and the transition between *closed* and *open* would be associated with the XB power stroke. In this scheme, cooperativity occurs within the span of a single RU as a result of a single *closed*-to-*open* transition from the power stroke of one XB facilitating the attachment of additional XBs within the thin filament span of the RU.

Thus, the kind of cooperativity whereby one XB holds an RU in an open state allowing other XBs to attach readily and proceed through a power stroke within the span of a single RU (Geeves and Lehrer, 1994; Lehrer, 1994; Tobacman, 1996) is somewhat different than the XB-XB and XB-RU cooperativity we represent here. Further differences would arise between the 3 RU-state configuration and our configuration in that, for instance, RU-RU interaction would impact both the *blocked*-to-*closed* transition and the *closed*-to-*open* transition rather than just the *on*-to-*off* transition. Whether one would arrive at different conclusions regarding the relative effects of RU-RU, XB-XB, and XB-RU neighbor interactions using the 3 RU-state model as opposed to the 2 RU-state model used in this study is a question worthy of future investigation.

Another noteworthy assumption is that Ca^{2+} binding and its effect on k_{on} and k_{off} were assumed to be independent of all other effects and of other actions associated with myofilament activation and cross-bridge cycling. There are both experimental evidence and theoretical reason for taking note of this assumption. Experimentally, Hoffmann and Fuchs (1987a,b) have shown in cardiac muscle that Ca^{2+} binds to myofilaments with less affinity at low force (vanadate inhibition), when there are fewer XBs in the force-bearing state, than at high force when there are more. Though not definitive, this evidence at least strongly implies that there is a dependence of Ca^{2+} binding on force-bearing XB state (Fuchs and Wang, 1995). Theoretically, a detailed balance, based on thermodynamic equilibrium considerations, demonstrates that our assignments of $k_{on}^{Ca} \gg k_{on}^{0}$ and $k_{off}^{Ca} \ll k_{off}^{0}$, while in accord with basic understanding of the influence of Ca^{2+} on the *on-off* transitions, are, nevertheless, inconsistent with one ratio of k^{+}/k^{-} for both *on* and *off* states. Indeed, T. L. Hill's thermodynamically consistent model of myofilament activation and cross-bridge cycling (Hill, 1985) specifically accounts for different Ca^{2+} binding affinities depending on whether the RU is *on* or *off*. In Hill's treatment, Ca^{2+} effects on equilibrium constants are not independent of other effects. Though respectful of experimental findings and thermodynamic constraints, we em-

ployed the Ca^{2+} binding assumption in our model because 1) we desired to examine specific neighbor interactions without the complications and obfuscations of multiple other effects, as would arise if Ca^{2+} interactions were included, and 2) the mathematics of including Ca^{2+} interactions may not be tractable in a model whose ultimate use will be for nonequilibrium applications during transient behaviors such as force development. Intuitively, we suspect that increases in Ca^{2+}-binding affinity with an increase in XB force-bearing states will, among the three neighbor interactions investigated here, have its greatest effect on the prediction of XB-RU interactions by shifting the force-log(Ca) curve farther to the left than would occur with XB-RU interaction alone. Suppose there is a certain level of XB-RU interaction and a resultant shift to the left of the force-pCa curve, as shown in Fig. 7. Now, if cooperative Ca^{2+} binding is imposed on top of existing XB-RU interaction, the result will be to shift the curve farther left. These two effects are in the same direction and if one is not considered but is operative, the other effect is overestimated. This means that if the effects of XB-dependent Ca^{2+} binding are operative and not considered, a larger value of w will be estimated than may actually exist as a result of XB-RU interaction alone. Future model improvements will be required to determine the effects of a dependence of Ca^{2+} binding affinity on XB state.

A third assumption of consequence was that states were assumed to be randomly distributed along the length of the myofilament, allowing the likelihood of finding a neighboring site in any particular state to be calculated according to its fractional occurrence. This assumption (used in formulating Eqs. 19, 29, and 44 in terms of Eqs. 20, 30, and 45, respectively) is at odds with neighbor interactions because these would tend to cluster states together in nonrandom patterns. Our assumption is known in statistical physics as the Bragg-Williams or mean-field approximation (Hill, 1978, 1985) where it is often used in solving neighbor interaction problems. An alternative is the Bethe-Peierls approximation (Hill, 1985) or quasi-chemical method in which spatial independence is not assumed and more exact solutions are obtained for one-dimensional, Ising-like problems of the kind treated here. However, in addition to being more complicated mathematically, the Bethe-Peierls approximation requires that all interactions be of the same strength. In our case, this requirement is not satisfied and, thus, the extra mathematical complexity is not warranted.

By employing the Bragg-Williams approximation, we retain a deterministic structure to the neighbor interaction problem and circumvent the requirement for probabilistic Monte Carlo methods in its solution. Deterministic model structures are desirable not only because they are less involved computationally, but also because they allow more straightforward explanations of cause and effect. The most important consequence of the Bragg-Williams approximation is that it exaggerates positive cooperativity (Hill, 1985). In our case, this exaggeration is of little consequence as the interaction parameters (u, v, or w) appear as free parameters whose values may be chosen in accord with the behavior the user wishes to simulate. That is, the model should be viewed as a tool in which the interaction strengths are assigned to represent system behavioral consequences, not as exact physical entities representing specific molecular interactions. However, through changes in parameter values, specific interactions may be graded accordingly.

Our assumption of randomly distributed states should be taken in the same light as Tobacman's comment (1996) about all previous cooperative models: "The cooperative mechanisms put into mathematical form by the models imply specific statistical distributions of myosin along the thin filament. Until methods are available for measuring those distributions, no model can be well substantiated and all models must be viewed with caution." The single relevant caution arising as a consequence of the Bragg-Williams approximation is that care be exercised to avoid large u, v, or w values that produce phase transition or critical point in the binding isotherm (i.e., force-pCa). Phase transition leads to a type of hysteresis that is uncharacteristic of the hysteresis in published force-pCa data (Harrison et al., 1988; Brandt et al., 1985). With this caveat, our assumption of random distribution is perfectly in accord with standard practices in solving neighbor interaction problems.

Model-based explanation of results

Maximal Ca^{2+}-activated force

The three types of neighbor interactions varied in their ability to increase F_{max}; increasing the strength of XB-XB neighbor interactions increased F_{max} approximately 6.5-fold, whereas increasing the strength of RU-RU or XB-RU interactions increased F_{max} only 30%. Differences between these effects may be explained as follows. The XB-XB interaction impacted the reaction step regulated by the f-f' rate-coefficient pair (Fig. 3 *B*) whereas RU-RU and XB-RU interactions impacted the reaction step regulated by the k_{on}-k_{off} rate-coefficient pair (Fig 3, *A* and *C*). The magnitude of F_{max} change resulting from either a change in f/f' or in k_{on}/k_{off} depended on the baseline fractional distribution among the various model states and differences in the size of the pool from which each of the affected reaction steps could potentially recruit more XBs into the force-bearing A_2 state.

The reference rate coefficients in Table 1 created conditions in which cycling XBs represented 75% of R_T ($\lambda^{cyc} = 0.75$), whereas XBs in the A_2 state represented only 6% of the total ($\lambda^{A_2} = 0.06$) and 8% of the cycling XBs ($\lambda^{A_2}_{cyc} = 0.08$). By subtraction, the noncycling R_{off} state represented only 25% of the total ($\lambda^{off} = 0.25$). Neighbor interactions may increase XBs in the A_2 state by two mechanisms: 1) by recruiting more XBs into the cycling population from R_{off}

and, thus, increasing λ^{cyc} and λ^{A_2} and 2) by redistributing the cross-bridges within the cycling population i.e. changing $\lambda^{A_2}_{cyc}$. Increases in RU-RU and XB-RU interactions acted to increase k_{on}/k_{off} (from a value of 2 at baseline when $u = w = 1$, to a value of 80 when $u = 1$ and $w = 5$, and to 17 when $u = 3$ and $w = 1$). These increases in k_{on}/k_{off} increased the cycling population λ^{cyc} (from $\lambda^{cyc} = 0.75$ at baseline to 0.99 when $u = 1$ and $w = 5$, and to 0.95 when $u = 3$ and $w = 1$) with a subsequent small increase in λ^{A_2} (to only 0.08) but without a change in $\lambda^{A_2}_{cyc}$ (remained at 0.08). The fact that the pool from which to recruit with k_{on}/k_{off} changes is limited to the 25% of actin-myosin sites in the baseline R_{off} state places a limit on the magnitude of the F_{max} change that can be induced. In contrast, the large increases in F_{max} achieved with XB-XB interaction arose because increasing v (from 1 to 3.2) caused an increase in f/f' (from 0.125 to 4.7), resulting in the redistribution within the cycling pool to favor A_2 formation (from $\lambda^{A_2}_{cyc} = 0.08$ at baseline to 0.40 when $v = 3.2$). Subsequent to this redistribution, there was a reduction in D with a secondary recruitment of XBs into the cycling population from R_{off} ($\lambda^{cyc} = 0.96$). Thus, the large increase in F_{max} with increased strength of XB-XB interaction resulted from the relatively large pool from which force-bearing XBs could be recruited.

If values for the reference rate coefficients other than those listed in Table 1 had been used in this study, results would have been quantitatively different, but the qualitative effects would have been much the same.

Steepness and symmetry

There were differences among the three types of neighbor interactions in their effect on the Ca^{2+}-dependent approach to F_{max} in the force-log(Ca/Ca_{50}) relationship. Whereas all three types of interaction shared the effect of increasing the steepness of the force-log(Ca/Ca_{50}) relationship, the RU-RU interaction easily had the greatest effect in this regard. Strong interaction between adjacent RUs created a condition that favored either all *off* or all *on*; if its neighbors were *off*, an RU tends to be held in the *off* position, but if its neighbors are *on* the RU tends to be held in the *on* position. In contrast, calcium binding promotes the transition from *off* to *on*. At low Ca^{2+} concentrations when most RU are *off*, neighbor interactions tend to hold the RU *off* even in the face of the weak effect of Ca^{2+} to promote the transition to *on*. These competing effects continue as Ca^{2+} concentrations are raised until there has been sufficient Ca^{2+}-induced transition to the *on* state that the neighbor interaction effects suddenly reverse and favor the transition to *on*. Thereafter with increasing Ca^{2+}, RU-RU interaction and Ca^{2+} activation act synergistically to both promote formation of the *on* state. Thus, if RU-RU interaction is sufficiently strong, there will be a very rapid switch-like transition with increasing Ca^{2+} from *off* (when neighbor interactions oppose Ca^{2+} activation) to *on* (when neighbor interactions act in the same direction as Ca^{2+} activation). This switch-like effect creates a steep force-log(Ca/Ca_{50}) curve.

The above argument also can be used to explain the asymmetry about $Ca^{2+} = Ca_{50}$ in the force-log(Ca/Ca_{50}) curve with strong RU-RU interactions. Note in Fig. 4 that when $u = 3$, the escape from zero baseline to higher values of F/F_{max} at low log (Ca/Ca_{50}) is slower ($n_H = 2$ for lower part of the curve) than the approach to $F/F_{max} = 1$ at higher log (Ca/Ca_{50}) ($n_H = 3$ for upper part of the curve). Thus, the force-log(Ca/Ca_{50}) curve is asymmetric about $F/F_{max} = 0.5$. This, too, is the result of RU-RU interactions opposing the activating effects of Ca^{2+} when $Ca^{2+} < Ca_{50}$ but supporting the activating effects of Ca^{2+} when $Ca^{2+} > Ca_{50}$. The resulting asymmetry made it difficult to characterize the steepness of the curve with a single Hill coefficient.

These effects with RU-RU interactions on force-log(Ca/Ca_{50}) symmetry were opposite to what was seen with XB-RU interactions. Note in Fig. 7 that when $w = 5$, the escape from zero to higher values of F/F_{max} at low log (Ca/Ca_{50}) is faster ($n_H = 3$ for lower part of the curve) than the approach to $F/F_{max} = 1$ at higher log (Ca/Ca_{50}) ($n_H = 1.5$ for upper part of the curve). The explanation for these differences derives from the differences in the changes in k_{on}/k_{off} ratio with Ca^{2+} in the presence of these different kinds of neighbor interactions.

In contrast, XB-XB interactions, which did not affect the k_{on}/k_{off} ratio with Ca^{2+}, produced a rather symmetric force-log(Ca/Ca_{50}) curve at all values of v. However, this curve could not be characterized with a single Hill coefficient; the curve in its middle range is much steeper than in the lower and the upper part (three-part value for the Hill coefficient was $n_H = 2, 7, 2$ for $v = 3.2$).

Left versus right shift

Increasing RU-RU and XB-XB interactions shifted the force-logCa relationship predominantly to the right (decrease in Ca^{2+} sensitivity), whereas increasing the XB-RU interaction shifted this relationship demonstrably to the left (increase in Ca^{2+} sensitivity). Of these effects, it is easiest to explain the leftward shift of XB-RU interactions as these interactions and Ca^{2+} activation work synergistically throughout the Ca^{2+} activation range to enhance activation by increasing the k_{on}/k_{off} ratio. Thus, the approach to activation saturation with increasing Ca^{2+} will be reached at lower Ca^{2+} concentrations with XB-RU interaction than without it and, consequently, the curve will be shifted left.

The rightward shift with RU-RU interaction follows from the above described mechanism for increased steepness; neighbor interactions act to hold an RU *off* if its neighbors are *off* at low Ca^{2+}, resulting in a rightward shift of the force-log(Ca/Ca_{50}) curve. For weak to modest XB-XB interaction ($v \leq 2.5$), the rightward shift for the normalized F/F_{max} curve may be misleading because, in terms of ab-

solute F, higher forces were achieved at lower Ca^{2+}. The rightward shift results from a greater relative expression of increasing force as Ca^{2+} saturation is approached compared to the condition of no XB-XB interaction. For greater strengths of XB-XB interaction ($v > 2.5$), there is a trend for leftward shift of the force-log(Ca/Ca_{50}) relationship because force saturation begins to occur before Ca^{2+} saturation.

Time course of force development

The three different types of neighbor interactions also differed in their effect on myofilament dynamics. Increasing the strength of XB-XB interactions had an obvious effect of slowing the characteristic rate of force development (Fig. 6), whereas increasing the strength of XB-RU interactions had an imperceptible effect at maximal Ca^{2+} activation but a perceptible effect to slow force development at low Ca^{2+} activation (data not shown).

An explanation of this apparent enigma whereby there is slowing of force development dynamics with increased cooperative interactions is found in a previous article (Campbell, 1997). In brief, the XB-XB interaction effect on f/f' ratio increases XBs in the A_2 state, i.e., it increases λ^{A_2}. It can be seen from Eq. 43 that when $v > 1$, an increase in λ^{A_2} also increases f/f'. Thus, a positive feedback between A_2 and f/f' is established where each enhances the other. If the pool for recruitment of A_2 is large, such positive feedback will slow system dynamics because it results in an ever-rising steady-state value during the course of force development. Indeed, from the standpoint of XB-XB interaction, the pool for A_2 recruitment is large as the pool resides in both the cycling XB population and the noncycling population. Thus, the positive feedback arising from the nonlinear dependence of f/f' on A_2 during XB-XB interaction produced an ever-advancing steady-state A_2, value and effectively slowed apparent system dynamics.

In contrast, XB-RU interactions, in acting to increase the k_{on}/k_{off} ratio, had little impact on the speed of force development. The pool for recruitment from the k_{on}/k_{off} reaction during maximal Ca^{2+} activation was small, consisting only of the noncycling state. Thus, for the same reason that these interactions had relatively small effects on F_{max}, they had relatively small effects on the speed of force development. When the noncycling pool was increased, as during half-maximal Ca^{2+} activation, XB-RU interactions perceptibly slowed force development, as would be predicted from the above analysis.

The situation with RU-RU interaction is more complex and depends strongly on initial conditions from which force development begins. Assume that $\lambda^{on} = 0$ is an initial condition. Then, for $u > 1$, the value of k_{on}/k_{off} at the onset of force development is less than that at baseline and remains less as long as $\lambda^{on} < 0.5$, Eq. 28. However, the value of k_{on}/k_{off} increases steeply as λ^{on} increases during force development and k_{on}/k_{off} quickly goes much above baseline as λ^{on} becomes greater than 1. These complicated effects of RU-RU interaction on k_{on}/k_{off} make it difficult to predict the time course of force development relative to a baseline time course. Early on, the time course is slower than baseline; as the eventual steady state is approached, it is faster. These complications made it difficult to interpret our observation of no perceptible effect of increased RU-RU interaction on speed of force development.

Even though the individual effects of RU-RU and XB-RU interactions cannot be detected in the rate of force development during maximum Ca^{2+} activation when they are each acting alone, both of these interactions significantly increased the speed of force development when they were added on top of XB-XB interaction effects which had acted to slow the speed of force development (Fig. 8).

The explanation for these results derives from the fact that the nonlinearities of neighbor interactions impact both the rate at which force develops and the final steady state to which force will eventually rise. These effects play out as follows. Consider the total number of available XBs, R_T, and the fraction of R_T that is force-generating and in the A_2 state, λ^{A_2}. At a given time, $t = t_0$, during force development, there will be a $\lambda^{A_{20}}$. Over the next increment in time, Δt, the time course of force development, proportional to $\lambda^{A_2}(t)$, may be closely approximated by

$$\lambda^{A_2}(t) = \lambda^{A_{2ss}}\left(1 - \frac{\lambda^{A_{2ss}} - \lambda^{A_{20}}}{\lambda^{A_{2ss}}}\, e^{-1/\tau}\right) \qquad (53)$$

where $\lambda^{A_{2ss}}$ is the projected steady state value of λ^{A_2} for continued exponential rise and τ is a time constant that characterizes the approach of $\lambda^{A_2}(t)$ to $\lambda^{A_{2ss}}$. If this expression accurately represented $\lambda^{A_2}(t)$ over the full time course of force development, $k_{dev} = 1/\tau$. The values of f, f', h, h', g, and k_{on}, and k_{off} at t_0 may be used to calculate effective values of both $\lambda^{A_{2ss}}$ and τ. These dependencies are such that $\lambda^{A_{2ss}}$ is bounded by the value 1 (i.e., no more than all of R_T may be committed to $\lambda^{A_{2ss}}$) while τ is bound by the value 0 (i.e., the approach to steady state may be infinitely fast).

Now according to Eq. 43, XB-XB interaction causes the f/f' ratio to increase progressively as $\lambda^{A_2}(t)$ increases. It can be shown that increasing f/f' increases $\lambda^{A_{2ss}}$ and decreases τ. Thus after the Δt interval, recalculation gives a larger $\lambda^{A_{2ss}}$ and a smaller τ and the trajectory given by Eq. 53 adjusts accordingly. If at $t = t_0$, $\lambda^{A_{2ss}} \ll 1$, we say that the pool for recruitment is large and after several Δt intervals, $\lambda^{A_{2ss}}$ continues to advance. In this case, the trajectory given by Eq. 53 repeatedly readjusts to chase an ever-advancing projected steady state. In spite of the fact that τ decreases, the net effect, as shown in Campbell (1997), is to slow the overall approach to steady state and to reduce the apparent k_{dev}. On the other hand, if at $t = t_0$, $\lambda^{A_{2ss}} \sim 1$, most of R_T is already committed to $\lambda^{A_{2ss}}$ and we say that the pool for recruitment is small. In this case, after Δt, recalculation will

give a new $\lambda^{A_{2ss}}$ that is not much different from the initial value. Under these conditions, the effect to decrease τ dominates and the result is to speed the overall approach to steady state and to increase the apparent k_{dev}. Therefore, whether neighbor interactions slow or speed force development and decrease or increase k_{dev} depends on the status of the pool from which new force-bearing XBs may be recruited.

Briefly, during XB-XB interaction, the dominant effect was the ever-advancing eventual steady state and, thus, there was slowing. However, when RU-RU and XB-RU interactions were added on top of these effects, the pool from which RU-RU and XB-RU interactions could recruit had already been depleted by XB-XB interaction. Thus, there was no opportunity to increase the eventual steady state, and the cooperative increase in rate coefficients dominated and rapidly brought the system to its final level. From these results we may conclude that whether slow-down or speed-up of the system occurs with cooperative neighbor interactions depends on which of the two nonlinearities is dominant, and this is determined by the relative size of the pool from which recruitment may occur. In turn, the latter is determined by the reference values of the parameters and baseline level of cooperative activity.

An interesting consequence of neighbor interactions (especially XB-XB interaction), related to the above argument, is that the rate of force development becomes Ca^{2+}-dependent (Fig. 9). Changing the calcium concentration changes the k_{on}/k_{off} ratio, which changes the size of the pool from which recruitment may occur. At high Ca^{2+} concentrations, the k_{on}/k_{off} ratio is high and the pool for recruitment is small. As Ca^{2+} concentration decreases, the k_{on}/k_{off} ratio also decreases and the pool for recruitment gets larger. With the increase in the recruitment pool there is a slowing of the force-redevelopment response, and the value of k_{dev} decreases with decreasing Ca^{2+} concentration. However, when Ca^{2+} concentrations become very small, to the point that k_{on}/k_{off} approaches zero, even highly cooperative systems become much less cooperative because there is no opportunity to carry out the cooperative action. Thus, for very low Ca^{2+} concentrations, k_{dev} increases to that of the noncooperative system.

Uses of optional neighbor interactions as hypotheses for mechanisms in experimental observations

The neighbor interactions examined here represent only a subset of the many possible mechanisms responsible for cooperative behavior in muscle contraction. Among potentially important cooperative mechanisms not considered here are those influencing Ca^{2+} binding to the RU and those that may arise from the stoichiometry whereby one RU regulates XB attachment to as many as 3 to 12 actin-myosin binding sites (Hill, 1985; Geeves and Lehrer, 1996). Thus, it should not be interpreted that the three kinds of neighbor interactions reported here are responsible for all observed cooperative behavior in contractile systems. Rather, these are mechanisms that can contribute to some currently unexplained contractile phenomena. As an example, we consider three of these phenomena.

Steepness and asymmetry in force-pCa relationship

The Hill coefficient, n_H, of the force-pCa curve varies widely for different types of muscle (Brandt et al., 1998). Traditionally, it has been understood that n_H of skeletal

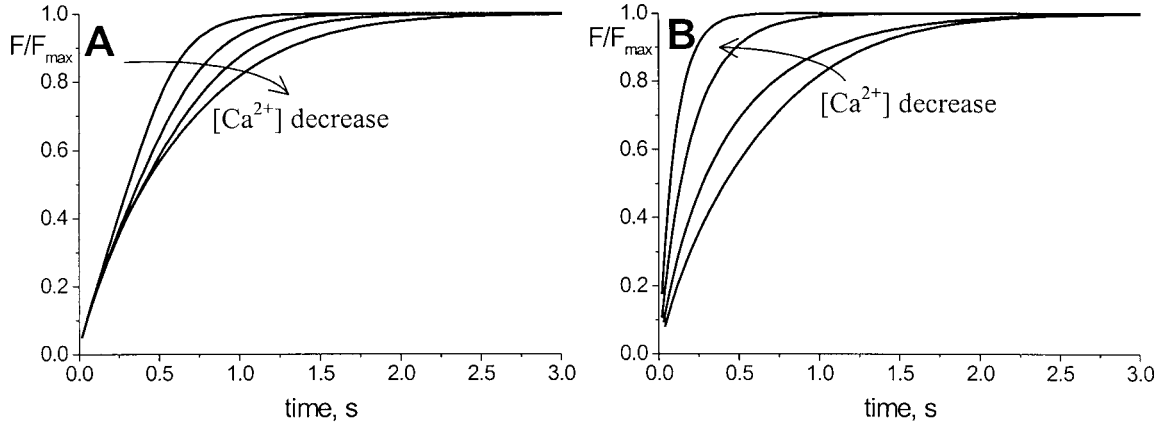

FIGURE 9 Neighbor interactions cause Ca^{2+}-dependent time course of force development. Neighbor interaction status for this figure was $\nu = 3$. (*A*) starting at near Ca^{2+} saturation ($Ca/Ca_{50} = 10$), progressive decreases in Ca^{2+} to $Ca/Ca_{50} = 1.5$ progressively slowed force development. Curves shown are for Ca/Ca_{50} of 10, 3, 2, and 1.5. However, further decreases of Ca^{2+} concentration (*B*, curves shown are for Ca/Ca_{50} of 1.5, 1, 0.5, and 0.1) increases the speed of force development. The data shown are for XB-XB interaction. Both RU-RU and XB-RU interaction gave qualitatively similar but quantitatively less pronounced results.

muscle (typically ≥ 5) was much higher than for cardiac muscle (typically 1–3), but recently values for cardiac muscle have been reported that were also ≥ 5 (Brandt et al., 1998; deTombe et al., 1996). Differences between skeletal and cardiac muscles can be a consequence of the different number of Ca^{2+} binding sites on the respective TnCs, but the possibility of differences due to variations in the strength of neighbor interactions in these muscles cannot be dismissed. Clearly, variations in the strength of any of the three neighbor interactions we examined here may be considered as mechanisms that account for variations in n_H between muscle types.

It has been reported that the force-pCa curve is asymmetric around the half maximum Ca^{2+} concentration (Moss, 1992). The force-pCa curve has a higher n_H in the range $pCa < pCa_{50}$ and a larger n_H in the range $pCa > pCa_{50}$. Among the three types of neighbor interactions, only XB-RU interaction produces this type of asymmetry. Therefore, the potential role of XB-RU interaction should be considered as a possible mechanism responsible for this asymmetric effect.

Ca^{2+} dependence of force development

An issue of considerable current interest is the Ca^{2+} dependence of the rate constant of force redevelopment, k_{dev}. Implicit in this interest is that Ca^{2+}-dependent k_{dev} is evidence that Ca^{2+} regulates XB kinetics (Brenner, 1988). Others have argued that a Ca^{2+}-dependent k_{dev} may actually be the result of cooperative feedback from the positive effects of force-bearing XB on thin-filament activation (Millar and Homsher, 1990; Swartz and Moss, 1992; Campbell, 1997). A consistent finding with skeletal muscle and the majority of findings with cardiac muscle indicate very little change or a decrease in k_{dev} for increasing activation levels yielding forces below half maximal force and then a severalfold increase in k_{dev}, with activation levels yielding forces above half maximal force (Vannier et al., 1996; Palmer and Kentish, 1998; Brandt et al., 1998; Brenner, 1988; Swartz and Moss, 1992; Metzger and Moss, 1990; Wolff et al., 1995; Hancock et al., 1996; Regnier et al., 1998).

The neighbor interactions we investigated demonstrated that XB-XB interaction brought about a decrease in k_{dev} with increasing Ca^{2+} during low levels of activation but an increase in k_{dev} with increasing Ca^{2+} at high level of activation (Fig. 9). Additionally, RU-RU and XB-RU interactions both had qualitatively the same kind of effect as that shown for XB-XB interaction in Fig. 9. Therefore, our results would lead to the hypothesis that Ca^{2+} dependence of rate of force development may be the result of one or more neighbor interaction effects.

Actions of Ca^{2+}-sensitizing agents

While many agents and experimental conditions have been observed to change F_{max}, not all observations can be explained by a known mechanism of action associated with these agents. For instance, a category of compounds referred to as the Ca^{2+}-sensitizing agents have a dramatic leftward shifting effect on the force-pCa curve and increase F_{max} (Lee and Allen, 1993; Solaro et al., 1993; Boukatina, 1998). There is no commonly accepted explanation for these effects. Among the three neighbor interactions investigated in this study, only increases in XB-RU interaction simultaneously produced a leftward shift in the force-logCa curve and an increase in F_{max}. XB-XB and RU-RU interactions, although increasing F_{max}, tended to shift the curve to the right. Because these latter actions are inconsistent with the effects of Ca^{2+} sensitizers as a class, induced changes in XB-XB and RU-RU interactions are unlikely mechanisms to explain Ca^{2+} sensitizer actions. However, agent-induced increases in XB-RU interactions remain a potential mechanism for explaining the action of the Ca^{2+} sensitizers.

SUMMARY

We describe the effects on model-predicted contraction behavior of three kinds of neighbor interactions within the myofilament system. Each produces a unique profile of contractile behaviors. Because the specific types of neighbor interactions have not been previously described, they have not been considered as possible mechanisms to explain experimental observations. Given the large number of unexplained contractile phenomena, it is now incumbent upon experimenters to consider these three types of neighbor interactions among the mechanisms that may be hypothesized to explain a wide array of observations.

REFERENCES

Brandt, P. W., F. Colomo, N. Piroddi, C. Poggesi, and C. Tesi. 1998. Force regulation by Ca^{2+} in skinned single cardiac myocytes of frog. *Biophys. J.* 74:1994–2004.

Brandt, P. W., M. S. Diamond, and F. H. Sachat. 1984. The thin filament of vertebrate skeletal muscle cooperatively activates as a unit. *J. Mol. Biol.* 180:379–384.

Brandt, P. W., M. S. Diamond, J. S. Rutchik, and F. H. Sachat. 1987. Co-operative interactions between troponin-tropomyosin units extend the length of the thin filament in skeletal muscle. *J. Mol. Biol.* 195: 885–896.

Brandt, P. W., B. Gluck, M. Mini, and C. Cerri. 1985. Hysteresis of the mammalian pCa/tension relation is small and muscle specific. *J. Musc. Res. Cell Motil.* 6:197–205.

Bremel, R. D., and A. Weber. 1972. Cooperation within actin filament in vertebrate skeletal muscle. *Nat. New Biol.* 238:97–101.

Brenner, B. 1988. Effect of Ca2+ on cross-bridge turnover kinetics in skinned single rabbit psoas fibers: implications for regulation of muscle contraction. *Proc. Natl. Acad. Sci. USA.* 85:3265–3269.

Bukatina, A. E., R. D. Kirkpatrick, and K. B. Campbell. 1998. Dethiophalloidin increases Ca2+ responsiveness of skinned cardiac muscle. *J. Musc. Res. Cell Motil.* 19:515–523.

Campbell, K. 1997. Rate constant of muscle force redevelopment reflects cooperative activation as well as cross-bridge kinetics. *Biophys. J.* 72: 254–262.

Daniels, T. L., A. C. Trimble, and P. B. Chase. 1998. Compliant realignment of binding sites in muscle: Transient behavior and mechanical tuning. *Biophys. J.* 74:1611–1621.

De Tombe, P. P., T. Wannenburg, D. Feng, and W. C. Little. 1996. Right ventricular contractile protein function in rats with left ventricular myocardial infarction. *Am. J. Physiol.* 271 (*Heart Circ. Physiol.* 40): H73–H79.

Dobrunz L. E., P. H. Backx, and D. T. Yue. 1995. Steady-state [Ca2+]i-force relationship in intact twitching cardiac muscle: direct evidence for modulation by isoproterenol and EMD 53998. *Biophys. J.* 69:189–201.

Fitzsimons, D. P., and R. L. Moss. 1998. Strong binding of myosin modulates length-dependent Ca2+ activation of rat ventricular myocytes. *Circ. Res.* 83:602–607.

Fuchs, F., and Y. P. Wang. 1996. Sarcomere length versus interfilament spacing as determinants of cardiac myofilament Ca^{2+} sensitivity and Ca^{2+} binding. *J. Mol. Cell Cardiol.* 28:1375–1383.

Geeves, M. A., and S. S. Lehrer. 1994. Dynamics of the muscle thin filament regulatory switch: the size of the cooperative unit. *Biophys. J.* 67:273–282.

Godt, R. 1974. Calcium-activated tension of skinned muscle fibers of the frog: dependence on magnesium adenosine triphosphate concentration. *J. Gen. Physiol.* 63:722–739.

Hancock, W. O., D. A. Martyn, L. L. Huntsman, and A. M. Gordon. 1996. Influence of Ca^{2+} on force redevelopment kinetics in skinned rat myocardium. *Biophys. J.* 70:2819–2829.

Harrison, S. M., C. Lamont, and D. J. Miller. 1988. Hysteresis and the length dependence of calcium sensitivity in chemically skinned rat cardiac muscle. *J. Physiol.* 401:115–143.

Hill, T. L. 1985. Cooperativity Theory in Biochemistry. Springer-Verlag, New York.

Hill, T. L., and L. Stein. 1978. Critical behavior of two-state, steady-state Ising system, according to the Bragg-Williams approximation. *J. Chem. Phys.* 69:1139–1150.

Hofmann, P. A., and F. Fuchs. 1987a. Effect of length and cross-bridge attachment on Ca^{2+} binding to cardiac troponin C. *Am. J. Physiol.* 253:C90–C96.

Hofmann, P. A., and F. Fuchs. 1987b. Evidence for a force-dependent component of calcium binding to cardiac troponin C. *Am. J. Physiol.* 253:C541–C546.

Lee, J. A., and D. G. Allen, eds. 1993. Modulation of Cardiac Calcium Sensitivity. Oxford University Press, New York.

Lehrer, S. S. 1994. The regulatory switch of the muscle thin filament: calcium or myosin heads? *J. Muscle Res. Cell Motil.* 15:232–236.

McKillop, D. F. A., and M. A. Geeves. 1993. Regulation of the interaction between actin and myosin subfragment 1. *Biophys. J.* 65:693–701.

Metzger, J. M., and R. L. Moss. 1990. Calcium-sensitive cross-bridge transitions in mammalian fast and slow skeletal muscle fibers. *Science* 247:1088–1090.

Mijailovich, S. M., J. J. Friedberg, and J. P. Butler. 1996. On the theory of muscle contraction: filament extensibility and the development of isometric force and stiffness. *Biophys. J.* 71:1475–1484.

Millar, N. C., and E. Homsher. 1990. The effect of phosphate and calcium on force generation in glycerinated rabbit skeletal muscle fibers: a steady-state and transient kinetic study. *J. Biol. Chem.* 265: 20234–20240.

Moss, R. L. 1992. Ca^{2+} regulation of mechanical properties of striated muscle. *Circ. Res.* 70:865–884.

Murray, J. M., and A. Weber. 1980. Cooperativity of the calcium switch of regulated actomyosin system. *Mol. Cell. Biochem.* 35:11–15.

Palmer, S., and J. C. Kentish. 1998. Roles of Ca^{2+} and cross-bridge kinetics in determining the maximum rates of Ca^{2+} activation and relaxation in rat and guinea pig skinned trabeculae. *Circ. Res.* 83: 179–186.

Pan, B. S., A. M. Gordon, and Z. Luo. 1989. Removal of tropomyosin overlap modifies cooperative binding of myosin S-1 to reconstituted thin filaments of rabbit striated muscle. *J. Biol. Chem.* 264:8495–8498.

Razumova, M. V., A. E. Bukatina, and K. B. Campbell. 1999. Stiffness-distortion sarcomere model for muscle simulation. *J. Appl. Physiol.* 87:1861–1876.

Regnier, M., D. A. Martyn, and P. B. Chase. 1998. Calcium regulation of tension redevelopment kinetics with 2-deoxy-ATP or low [ATP] in rabbit skeletal muscle. *Biophys. J.* 74:2005–2015.

Rice, J. R., R. L. Winslow, and W. C. Hunter. 1999. Comparison of putative cooperative mechanisms in cardiac muscle: length dependence and dynamic responses. *Am. J. Physiol.* 276 (*Heart Circ. Physiol.* 45): H1734–H1754.

Solaro, R. J., G. Gambassi, D. M. Warshaw, M. R. Keller, H. A. Spurgeon, N. Beier, and E. G. Latkata. 1993. Stereoselective actions of thiadiazinones on canine cardiac myocytes and myofilaments. *Circ. Res.* 73: 981–990.

Solaro, R. J., and H. M. Rarick. 1998. Troponin and tropomyosin: proteins that switch on and tune in the activity of cardiac myofilaments. *Circ. Res.* 83:471–480.

Squire, J. M., and E. P. Morris. 1998. A new look at thin filament regulation in vertebrate skeletal muscle. *FASEB J.* 12:761–771.

Swartz, D. R., M. L. Greaser, and R. L. Moss. 1996. Calcium alone does not fully activate the thin filament for S1 binding in rigor myofibrils. *Biophys. J.* 71:1891–1904.

Swartz, D. R., and R. L. Moss. 1992. Influence of a strong-binding myosin analogue on calcium-sensitive mechanical properties of skinned skeletal muscle fibers. *J. Biol. Chem.* 267:20497–20506.

Swartz, D. R., D. Zhang, and K. W. Yancey. 1999. Cross bridge-dependent activation of contraction in cardiac myofibrils at low pH. *Am. J. Physiol.* 276(*Heart Circ. Physiol.* 45):H1460–H1467.

Tobacman, L. S. 1996. Thin filament mediated regulation of cardiac contraction. *Annu. Rev. Physiol.* 58:447–481.

Vannier, C., H. Chevassus, and G. Vassort. 1996. Ca-dependence of isometric force kinetics in single skinned ventricular cardiomyocytes from rats. *Cardiovasc. Res.* 32:580–586.

Wolff, M. R., K. S. McDonald, and R. L. Moss. 1995. Rate of tension development in cardiac muscle varies with level of activator calcium. *Circ. Res.* 76:154–160.

Zou, G., and G. N. Phillips. 1994. A cellular automaton model for the regulatory behavior of muscle thin filaments. *Biophys. J.* 67:11–28.